Nonlinear Dynamic Analysis of Shells of Revolution by Matrix Displacement Method

J. A. STRICKLIN,* J. E. MARTINEZ,† J. R. TILLERSON,‡ J. H. HONG,§ and W. E. HAISLER¶
Texas A&M University, College Station, Texas

A formulation and computer program is developed for the geometrically nonlinear dynamic analysis of shells of revolution under symmetric and asymmetric loads. The nonlinear strain energy expression is evaluated using linear functions for all displacements. Five different procedures are examined for solving the equations of equilibrium, with Houbolt's method proving to be the most suitable. Solutions are presented for the symmetrical and asymmetrical buckling of shallow caps under step pressure loadings and a wide variety of other problems including some highly nonlinear ones.

Nomenclature

⌊ ⌋ = row matrix
[ ] = square matrix
{ } = column matrix
[ ]′ = matrix transpose
C_1 = $E_s t/(1 - \nu_{s\theta}\nu_{\theta s})$
C_2 = $E_\theta t/(1 - \nu_{s\theta}\nu_{\theta s})$
D_1 = $E_s t^3/[12(1 - \nu_{s\theta}\nu_{\theta s})]$
D_2 = $E_\theta t^3/[12(1 - \nu_{s\theta}\nu_{\theta s})]$
E = Young's modulus
$\hat{e}$ = linear strains and rotations
F = pressure loading on shell
G = shear modulus
G_1 = Gt
G_2 = $Gt^3/12$
$[K]$ = stiffness matrix
L = meridional length of shell element
$[M]$ = mass matrix
$\{Q\}$ = generalized forces
$\{q\}$ = nodal displacements
r = cylindrical coordinate
s = meridional distance along shell element
t = shell thickness and time
T = kinetic energy
U = internal energy
u,v,w = displacements in meridional, circumferential and normal directions, respectively
Δt = time increment
ϵ = midsurface strains
θ = circumferential angle
ν = Poisson's ratio
ϕ = slope of undeformed shell
ϕ' = $d\phi/ds$
χ = changes in curvature

Superscripts and Subscripts

e = element
L = linear and at $s = L$
NL = nonlinear
m = middle of element and degree of freedom of element
n = harmonic number
o = initial value and at $s = 0$
s = meridional direction
θ = circumferential direction

Presented as paper at the AIAA/ASME 11th Structures, Structural Dynamics, and Materials Conference, Denver, Colo., April 22–24, 1970 (no paper number; published in bound volume); submitted June 10, 1970; revision received November 23, 1970. Research supported under Sandia Contract 82-3683 and NASA Grant NGL-44-001-004. Appreciation is expressed to W. Von Riesemann of Sandia and F. Stebbins of Manned Spacecraft Center, who served as technical monitors for the research. Appreciation is also expressed to S. Key and R. Krieg of Sandia for their helpful suggestions during the course of this research.

* Professor, Department of Aerospace Engineering. Member AIAA.
† Assistant Professor, Department of Civil Engineering. Member AIAA.
‡ Research Assistant, Department of Aerospace Engineering. Associate Member AIAA.
§ Research Assistant, Department of Aerospace Engineering.
¶ Assistant Professor, Department of Aerospace Engineering. Associate Member AIAA.

Introduction

THE geometrically nonlinear static analysis of structures has made considerable progress since the original finite element paper by Turner, Dill, Martin, and Melosh.[1] In Ref. 1, it was proposed that the nonlinear problem be analyzed as a sequence of linear problems using a geometric stiffness matrix. This approach has been used by many investigators in more recent years and has been refined to a very high degree. In fact, it is safe to say that the geometric stiffness method approach is the most widely used method for the geometrically nonlinear analysis of structures by the matrix displacement method with the Newton-Raphson method of solution being a distant second. Rather exhaustive survey articles on the nonlinear analysis of structures by matrix methods have been presented by Martin[2] and Oden.[3]

For a shell of revolution under asymmetrical loading, the incremental stiffness method is difficult to apply due to the coupling that the nonlinear terms introduce among the various Fourier harmonics. This gives rise to a large number of equations which must be solved after new coefficients are generated at each load increment. For example, twenty harmonics and fifty elements would give rise to 4080 equations of equilibrium.

The difficulty of repeated solutions of a large number of equations has been circumvented by Stricklin, Haisler, MacDougall, and Stebbins[4] who place the nonlinear terms on the right-hand side of the equations of equilibrium and treat them as additional loads. The method of solution is by iteration and has been found to yield accurate results for a large majority of practical problems. For highly nonlinear problems, the equations as formulated in Ref. 4 are currently being solved by the Newton-Raphson procedure, with the coupling between harmonics being ignored when the nonlinear terms are treated as pseudo loads and taken to the right-hand side of the equations. The present paper presents an extension of the work presented in Ref. 4 to the nonlinear dynamic analysis of shells of revolution under both symmetric and asymmetric loadings. It will be demonstrated that the approach presented herein is valid for highly nonlinear problems. It is assumed in the present work that the material is elastic and nonlinearities are due to moderate rotations.

Computer programs for the large deflection elastic-plastic analysis of beams, rings, and plates have been developed by Witmer, Balmer, Leech, and Pian[5] and Krieg and Duffey.[6] In Refs. 5 and 6, the governing equations of motion are written in finite-difference form in both space and time. The solution is straight forward in that the equations are solved sequentially with no coupling existing between equations. Correlation studies have been conducted by Duffey and Key,[7] Krieg, Duffey, and Key,[8] and Balmer and Witmer.[9] The correlation studies have demonstrated that the computer programs as described in Refs. 5 and 6 may be used to compute the large deflection dynamic response of highly nonlinear elastic-plastic simple structures.

Leech, Witmer, and Pian[10] and Wrenn, Sobel, and Silsby[11] have presented formulations and computer programs for the nonlinear analysis of general thin shells. The equations governing the response of a shell under arbitrary impulsive loading are developed in tensor form and represented by finite differences in space and time. Solutions are presented for a cylindrical panel[10] and a cylinder.[11] In addition to finite differences in time, the Adams-Moulton and fourth-order Runge-Kutta methods were used in Ref. 11. An interesting conclusion drawn in Ref. 11 is that the size of the time increment needed for numerical stability in the finite difference method of solution is smaller than the time increment needed to prevent excessive truncation error.

Stability studies on the different methods used to approximate the second derivatives in time have recently been conducted by Leech, Hsu, and Mack,[12] Johnson,[13] Krieg,[14] and Nickell.[15] However, with the exception of Ref. 14, the studies have been limited to the linear equations of motion and are not applicable to the nonlinear analysis. In particular, the unconditional stability exhibited by Houbolt's[13] and Newmark's[15] ($\gamma = \frac{1}{2}$, $\beta = \frac{1}{4}$) methods for the linear case does not exist in the nonlinear formulation presented in this paper.

It is apparent from the cited references that considerable progress has been made in analyzing the elastic-plastic nonlinear dynamic behavior of shells using finite differences in the spatial coordinates. However, little progress has been made in the analysis of the nonlinear dynamic behavior of shells through the finite element approach. Further, there does not seem to exist any computer program which is capable of analyzing the nonlinear asymmetrical dynamic behavior of shells of revolution in a reasonable period of computer time. The purpose of the present paper is to present such a program and demonstrate through examples its range of applicability.

The research presented here uses the curved element of Stricklin, Navaratna, and Pian[16] and the displacement function of Grafton and Strome.[17] The nonlinear shell theory of Novozhilov[18] is assumed to be applicable with the further assumption of small strains and moderate rotations being made. Reference 4 presents a more complete review of the pertinent literature and a detailed description of the theoretical formulation. However, missing from Ref. 4 are the discussions of the works on the linear dynamic anaysis of shells of revolution by Klein and Sylvester[19] and Popov and Chow.** Klein and Sylvester use the method of Chan, Cox, and Benfield[20] to solve the equations of equilibrium whereas Popov and Chow use the modal analysis. The results obtained by both methods which are presented in Ref. 19 are in good agreement for a spherical cap under a step pressure loading. This same problem is analyzed herein and the results are presented in a later section.

In the earlier stages of the research presented herein, the method of Ref. 20 was used for solutions. In fact, a Technical Note[21] has been published on the axisymmetric dynamic buckling of shallow caps under step pressure loading in which the method of Ref. 20 was used to solve the equations of equilibrium. However, more recent studies have shown that Houbolt's method[22] is more stable and thereby more efficient than the method of Ref. 20 for solving highly nonlinear problems. Consequently, most of the results presented in this report are based on Houbolt's method of solution.

** Presented as Addendum in Ref. 19.

Formulation

The matrix displacement method is an energy formulation and, consequently, the equations of equilibrium for the nonlinear dynamic response are obtained from Lagrange's equation:

$$d/dt(\partial T/\partial \dot{q}_i^n) + \partial U/\partial q_i^n = Q_i^n \tag{1}$$

where q_i^n = generalized degree of freedom i in harmonic n.

In the present formulation the internal energy is separated into two parts:

$$U = U_L + U_{NL} \tag{2}$$

where U_L = strain energy based on linear strain displacement relations; U_{NL} = strain energy contribution due to the inclusion of nonlinearities in strain displacement relations.

Substituting Eq. (2) into Eq. (1) and taking the nonlinear strain energy expression to the right-hand side, the equations of equilibrium become

$$[M^n]\{\ddot{q}^n\} + [K^n]\{q^n\} = \{\boldsymbol{Q}^n\} - \{\partial U_{NL}/\partial q^n\} \tag{3}$$

It should be noted that Eq. (3) is valid for any harmonic n with the coupling between harmonics appearing in the last term on the right-hand side. The remainder of this section presents a discussion of the various terms in Eq. (3).

Strain Energy

The strain energy expression valid for orthotropic shells is given by[23]

$$U = \tfrac{1}{2}\iint(C_1\epsilon_s^2 + C_2\epsilon_\theta^2 + 2\nu_{s\theta}C_1\epsilon_s\epsilon_\theta + G_1\epsilon_{s\theta}^2 + D_1\chi_s^2 + D_2\chi_\theta^2 + 2\nu_{s\theta}D_1\chi_s\chi_\theta + G_2\chi_{s\theta}^2)rdsd\theta \tag{4}$$

Restricting the equation given by Novozhilov[18] to shells of revolution and assuming only moderate rotations, the strains and curvatures are given by

$$\epsilon_s = \hat{e}_s + \tfrac{1}{2}\,\hat{e}_{13}^2 \quad \epsilon_\theta = \hat{e}_\theta + \tfrac{1}{2}\,\hat{e}_{23}^2 \tag{5a}$$

$$\epsilon_{s\theta} = \hat{e}_{s\theta} + \hat{e}_{13}\hat{e}_{23} \quad \chi_s = -\partial\hat{e}_{13}/\partial s \tag{5b}$$

$$\chi_\theta = -(1/r)(\partial\hat{e}_{23}/\partial\theta) - (1/r)\sin\phi\,\hat{e}_{13}$$

$$\chi_{s\theta} = -(1/r)(\partial\hat{e}_{13}/\partial\theta) + (\sin\phi/r)\hat{e}_{23} - \partial\hat{e}_{23}/\partial s \tag{6}$$

where

$$\hat{e}_s = (\partial u/\partial s) - \phi' w \tag{7a}$$

$$\hat{e}_\theta = (1/r)[(\partial v/\partial\theta) + u\sin\phi + w\cos\phi] \tag{7b}$$

$$\hat{e}_{s\theta} = (1/r)(\partial u/\partial\theta) - (v/r)\sin\phi + \partial v/\partial s \tag{7c}$$

$$\hat{e}_{13} = (\partial w/\partial s) + u\phi' \tag{7d}$$

$$\hat{e}_{23} = (1/r)(\partial w/\partial\theta) - (v\cos\phi)/r \tag{7e}$$

Substituting Eq. (5) into Eq. (4) allows the strain energy expression to be separated into two parts given by Eq. (2). U_L is the usual expression for the internal energy based on linear theory and is obtained by replacing the ϵ's in Eq. (4) by the corresponding $\hat{e}$'s. The internal energy due to nonlinearities in the strain displacement relation is given by

$$U_{NL} = \tfrac{1}{2}\iint[C_1\hat{e}_s\hat{e}_{13}^2 + C_2\hat{e}_\theta\hat{e}_{23}^2 + \nu_{s\theta}C_1(\hat{e}_s\hat{e}_{23}^2 + \hat{e}_\theta\hat{e}_{13}^2) + 2G_1\hat{e}_{s\theta}\hat{e}_{13}\hat{e}_{23}]\,rdsd\theta + \tfrac{1}{2}\iint[\tfrac{1}{4}C_1\hat{e}_{13}^4 + \tfrac{1}{4}C_2\hat{e}_{23}^4 + (\tfrac{1}{2}\nu_{s\theta}C_1 + G_1)\hat{e}_{13}^2\hat{e}_{23}^2]\,rdsd\theta \tag{8}$$

It is noted that the fourth-order terms in the $\hat{e}$'s have been included in Eq. (8) as recent results[21] have shown them absolutely essential for accurate results.

Displacement Function††

The basic criteria which the displacement functions should satisfy[24] is that if the internal energy is a function of the jth derivative of the displacements then continuity of the $(j - 1)$th derivative should be satisfied between elements. The strain energy expression based on linear theory depends on the second derivative of w, but the strain energy expression due to nonlinearities depends on the first derivative only. Thus, it is permissible to use different displacement functions for w in the evaluation of U_L and U_{NL}. The assumed displacement functions which satisfy the necessary conditions are: a) in U_L;

$$w = \sum_{i=0} \left[\left(1 - \frac{3s^2}{L^2} + \frac{2s^3}{L^3}\right)\bar{q}_3^{\,i} + \left(s - \frac{2s^2}{L} + \frac{s^3}{L^2}\right)(q_4^{\,i} - \bar{q}_1\phi') + \left(\frac{3s^2}{L^2} - \frac{2s^3}{L^3}\right)\bar{q}_7^{\,i} + \left(-\frac{s^2}{L} + \frac{s^3}{L^2}\right)(q_8^{\,i} - \bar{q}_5\phi_L')\right]\cos i\theta \tag{9}$$

b) in U_{NL};

$$w = \sum_{i=0} \left[\left(1 - \frac{s}{L}\right)\bar{q}_3^{\,i} + \bar{q}_7^{\,i}\,\frac{s}{L}\right)\Big]\cos i\theta \tag{10}$$

and c) in U_L and U_{NL};

$$u = \sum_{i=0} \left[\left(1 - \frac{s}{L}\right)\bar{q}_1^{\,i} + \bar{q}_5^{\,i}\,\frac{s}{L}\right]\cos i\theta \tag{11a}$$

$$v = \sum_{i=0} \left[\left(1 - \frac{s}{L}\right)\bar{q}_2^{\,i} + \bar{q}_6^{\,i}\,\frac{s}{L}\right]\sin i\theta \tag{11b}$$

where

$$\bar{q}_1 = q_1\cos\phi_0 + q_3\sin\phi_0 \tag{12a}$$

$$\bar{q}_3 = -q_1\sin\phi_0 + q_3\cos\phi_0 \tag{12b}$$

$$\bar{q}_5 = q_5\cos\phi_L + q_7\sin\phi_L \tag{12c}$$

$$\bar{q}_7 = -q_5\sin\phi_L + q_7\cos\phi_L \tag{12d}$$

The $\bar{q}$'s simply represent the displacements in shell coordinates. It is noted that symmetry about $\theta = 0$ is assumed in the displacement function in u and w. Cubic displacement functions in u and v as presented in Ref. 25 are employed in the present version of the computer code to better approximate rigid-body motion.

In the computer code, a maximum of five harmonics may be chosen in the expansion. These five harmonics may be selected arbitrarily from the first twenty harmonics provided harmonic zero is included.

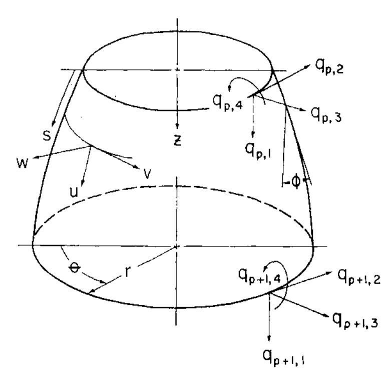

Fig. 1 Generalized coordinates of shell element.

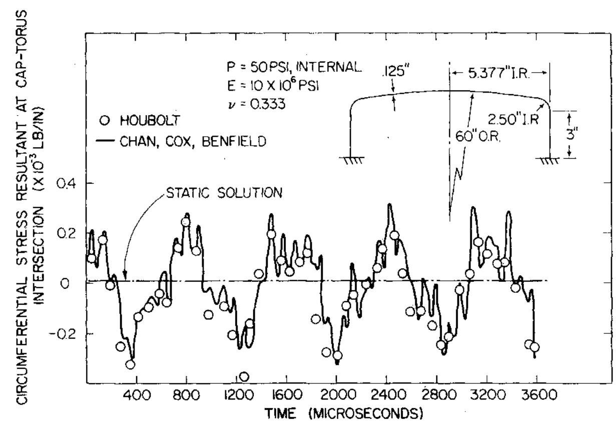

Fig. 2 Circumferential stress resultant for shell under step pressure loading.

Pseudo Nonlinear Forces

The pseudo generalized forces for an element are obtained by taking the partial derivative of the strain energy expression due to nonlinearities [Eq. (8)] with respect to the generalized coordinates of the element (Fig. 1). This yields

$$\frac{\partial U_{NL}}{\partial q_m^{\,n}} = \frac{1}{2}\iint \Big\{(C_1\hat{e}_{13}^2 + \nu_{s\theta}C_1\hat{e}_{23}^2)\frac{\partial \hat{e}_s}{\partial q_m^{\,n}} + (C_2\hat{e}_{23}^2 + \nu_{s\theta}C_1\hat{e}_{13}^2)\frac{\partial \hat{e}_\theta}{\partial q_m^{\,n}} + 2G_1\hat{e}_{13}\hat{e}_{23}\frac{\partial \hat{e}_s}{\partial q_m^{\,n}} + (2C_1\hat{e}_s\hat{e}_{13} + 2\nu_{s\theta}C_1\hat{e}_\theta\hat{e}_{13} + 2G_1\hat{e}_{s\theta}\hat{e}_{23})\frac{\partial \hat{e}_{13}}{\partial q_m^{\,n}} + (2C_2\hat{e}_\theta\hat{e}_{23} + 2\nu_{s\theta}C_1\hat{e}_s\hat{e}_{23} + 2G_1\hat{e}_{s\theta}\hat{e}_{13})\frac{\partial \hat{e}_{23}}{\partial q_m^{\,n}}\Big\}\, r ds d\theta + \frac{1}{2}\iint \Big\{[C_1\hat{e}_{13}^3 + (\nu_{s\theta}C_1 + 2G_1)\,\hat{e}_{13}\hat{e}_{23}^2]\frac{\partial \hat{e}_{13}}{\partial q_m^{\,n}} + [C_2\hat{e}_{23}^3 + (\nu_{s\theta}C_1 + 2G_1)\,\hat{e}_{13}^2\hat{e}_{23}]\frac{\partial \hat{e}_{23}}{\partial q_m^{\,n}}\Big\}\, r d\theta ds \tag{13}$$

For an efficient computer code, Eq. (13) must be evaluated without the use of auxiliary storage in the computer and for this reason, linear functions (in S) for the displacements u, v, and w, are used. Another assumption made in the evaluation of Eq. (13) is that the integrals over the meridional length of the element may be evaluated through strip integration. The integrals in the circumferential direction are evaluated in closed form for the particular harmonics chosen.

Substituting Eqs. (10) and (11) into Eq. (7) and evaluating the results at the center of the element, the strains and rotations become

$$\hat{e}_s = \sum_{i=0} e_s^{\,i}\cos i\theta \qquad \hat{e}_\theta = \sum_{i=0} e_\theta^{\,i}\cos i\theta \tag{14a}$$

$$\hat{e}_{s\theta} = \sum_{i=0} e_{s\theta}^{\,i}\sin i\theta \qquad \hat{e}_{13} = \sum_{i=0} e_{13}^{\,i}\cos i\theta \tag{14b}$$

$$\hat{e}_{23} = \sum_{i=0} e_{23}^{\,i}\sin i\theta \tag{14c}$$

where

$$e_s^{\,i} = \frac{\bar{q}_5^{\,i} - \bar{q}_1^{\,i}}{L} - \frac{\bar{q}_7^{\,i} + \bar{q}_3^{\,i}}{2}\,\phi'_m \tag{15a}$$

$$e_\theta^{\,i} = \frac{1}{r_m}\left(i\,\frac{q_2^{\,i} + q_6^{\,i}}{2} + \frac{\bar{q}_1^{\,i} + \bar{q}_5^{\,i}}{2}\sin\phi_m + \frac{\bar{q}_3^{\,i} + \bar{q}_7^{\,i}}{2}\cos\phi_m\right) \tag{15b}$$

†† Conical frustrum elements are used for the nonlinear terms only (March 10, 1971).

$$e_{s\theta}{}^i = -i\,\frac{\bar{q}_5{}^i + \bar{q}_1{}^i}{2r_m} - \frac{q_2{}^i + q_6{}^i}{2r_m}\sin\phi_m + \frac{q_6{}^i - q_2{}^i}{L} \quad (15c)$$

$$e_{13}{}^i = \frac{\bar{q}_7{}^i - \bar{q}_3{}^i}{L} + \frac{\bar{q}_1{}^i + \bar{q}_5{}^i}{2}\,\phi'_m \quad (15d)$$

$$e_{23}{}^i = \frac{1}{r_m}\left[-i\left(\frac{\bar{q}_7{}^i + \bar{q}_3{}^i}{2}\right) - \frac{q_2{}^i + q_6{}^i}{2}\cos\phi_m\right] \quad (15e)$$

Substituting Eqs. (14) into Eq. (13) and using strip integration over the length, Eq. (13) becomes

$$\frac{\partial U_{\mathrm{NL}}}{\partial q_m{}^n} = \frac{r_m L}{2}\sum_{i=0}\sum_{j=0}\Big\{(C_1{}^{ijn}e_{13}{}^i e_{13}{}^j + \nu_{s\theta}\,C_1{}^{\bar{i}\bar{j}n}e_{23}{}^i e_{23}{}^j) \times \frac{\partial e_s{}^n}{\partial q_m{}^n} + (C_2{}^{\bar{i}\bar{j}n}e_{23}{}^i e_{23}{}^j + \nu_{s\theta}C_1{}^{ijn}e_{13}{}^i e_{13}{}^j)\frac{\partial e_\theta{}^n}{\partial q_m{}^n} + 2G_1{}^{i\bar{j}\bar{n}}e_{13}{}^i e_{23}{}^j\frac{\partial e_{s\theta}{}^n}{\partial q_m{}^n} + (2C_1{}^{ijn}e_s{}^i e_{13}{}^j + 2\nu_{s\theta}C_1{}^{ijn}e_\theta{}^i e_{13}{}^j + 2G_1{}^{\bar{i}\bar{j}n}e_{s\theta}{}^i e_{23}{}^j)\frac{\partial e_{13}{}^n}{\partial q_m{}^n} + (2C_2{}^{i\bar{j}\bar{n}}e_\theta{}^i e_{23}{}^j + 2\nu_{s\theta}C_1{}^{i\bar{j}\bar{n}}e_s{}^i e_{23}{}^j + 2G_1{}^{\bar{i}j\bar{n}}e_{s\theta}{}^i e_{13}{}^j)\frac{\partial e_{23}{}^n}{\partial q_m{}^n}\Big\} + \frac{r_m L}{2}\sum_{i=0}\sum_{j=0}\sum_{k=0}\Big\{[C_1{}^{ijkn}e_{13}{}^i e_{13}{}^j e_{13}{}^k + (\nu_{s\theta}C_1{}^{i\bar{j}\bar{k}n} + 2G_1{}^{i\bar{j}\bar{k}n})\,e_{13}{}^i e_{23}{}^j e_{23}{}^k]\frac{\partial e_{13}{}^n}{\partial q_m{}^n} + [C_2{}^{\bar{i}\bar{j}\bar{k}\bar{n}}e_{23}{}^i e_{23}{}^j e_{23}{}^k + (\nu_{s\theta}C_1{}^{ij\bar{k}\bar{n}} + 2G_1{}^{ij\bar{k}\bar{n}})\,e_{13}{}^i e_{13}{}^j e_{23}{}^k]\frac{\partial e_{23}{}^n}{\partial q_m{}^n}\Big\} \quad (16)$$

where r_m = value of r at middle of element; L = length of element. The superscripts over the material constants, C_1, C_2, G_1 indicate that the material constant is multiplied by the integral of the trigonometric function. For example,

$$C_1{}^{ijkn} = C_1\int_0^{2\pi}\cos i\theta\,\cos j\theta\,\cos k\theta\,\cos n\theta\,d\theta \quad (17)$$

A bar over i, j, k, or n indicates that $\cos\theta$ is replaced by $\sin\theta$ in the integral.

For known values of the displacements, Eq. (16) is evaluated for each and every element of the structure. The result is a set of forces for the element which are combined in the usual way to obtain the generalized forces for the shell.

Mass Matrix

The mass matrix for the shell is evaluated from the kinetic energy expression and includes the effect of rotary inertia.

Methods of Solution

The numerical methods of solution which have been used to calculate the nodal displacements of the shells under study are discussed in this section. Three independent methods have been utilized with one of the methods being varied to provide a total of five different numerical solution schemes. The formulation of these methods for use in solving the shell equations is presented in Ref. 26, and the results obtained using each method are discussed. Additional methods of solution are also presented in this reference.

The equations of motion, Eq. (3) can be reduced to a system of equations of the form

$$[M]\{\ddot{q}\} + [K]\{q\} = \{F(t,q)\} \quad (18)$$

The load matrix, $\{F(t,q)\}$, is equivalent to the right-hand side of Eq. (3). The numerical schemes discussed are formulated to satisfy these governing differential equations of motion.

Houbolt's Method

The finite difference method of solution developed by Houbolt[22] for use in dynamic structural response studies of aircraft can be adapted for use in determining the dynamic nonlinear response of shells of revolution. The accelerations in Eq. (18) are replaced by a finite difference approximation of the second derivative. This substitution allows development of recurrence relations which can be used for the step-by-step calculation of the displacements of the shell.

Levy and Kroll[27] and Johnson and Greif[28] have used Houbolt's procedure to solve dynamical problems. These researchers conclude that this procedure will yield good results if the time increment is less than $\frac{1}{30}$ of the period of the highest frequency mode.

The accelerations of the nodes of the shell are approximated by the third-order backwards difference expression,

$$\{\ddot{q}_{n+1}\} = 1/(\Delta t)^2\{2q_{n+1} - 5q_n + 4q_{n-1} - q_{n-2}\} \quad (19)$$

The accuracy of this representation is of the order $(\Delta t)^2$.

Substituting Eq. (19) into Eq. (18) and simplifying yields

$$\{2[M] + (\Delta t)^2[K]\}\{q_{n+1}\} = (\Delta t)^2\{F(t,q)_{n+1}\} + [M]\{5q_n - 4q_{n-1} + q_{n-2}\} \quad (20)$$

This equation is valid for all time increments but must be modified for the first step. The starting procedure is the same one recommended by Houbolt.[22]

Approximation of Loads Matrix

Both the method of Houbolt and the Chan, Cox, and Benfield method[20,29] require that the loads at the end of the $(n + 1)$th time increment be known in order to calculate the displacements at the end of that increment. These loads, because of the presence of the nonlinear terms, are a function of the displacements which are to be calculated. It is therefore not possible to evaluate these terms exactly.

Consequently, the right-hand side of Eq. (18) was evaluated using a first-order Taylor's series expanded about the nth time increment:

$$\{F(t,q)_{n+1}\} = \{F(t,q)_n\} + \partial/\partial t\{F(t,q)_n\}\Delta t \quad (21)$$

Approximating the partial derivative by a first-order backwards difference expression gives

$$\{F(t,q)_{n+1}\} \simeq 2\{F(t,q)_n\} - \{F(t,q)_{n-1}\} \quad (22)$$

This expression has an inherent error of order $(\Delta t)^2$ which is the same as the order of error inherent in both the Houbolt and the Chan, Cox, and Benfield[20] solutions. It corresponds to a linear extrapolation of the loads at the two previous time increments.

Runge-Kutta Evaluation

A shallow spherical cap with clamped edges was analyzed using the Runge-Kutta[30] method of solution. The cap was subjected to an instantaneously applied (at time = 0) internal pressure. Only the zero harmonic response was determined.

Linear solutions of the problem were numerically unstable for time increments of 2.0×10^{-6}, and 0.5×10^{-6} sec. This instability consistently occurred after only a few time steps had been taken. The time increment was further reduced to the very small value of 0.5×10^{-8} sec, and the solution obtained did not exhibit any numerical instability. Utilizing this extremely small time increment would require prohibitive amounts of computer time to determine the response of a shell.

Chan, Cox, and Benfield Solution ($\beta = \frac{1}{6}$ and $\beta = 0$)

For a variety of problems, attempts were made to calculate the response curves using both $\beta = 0$ and $\beta = \frac{1}{6}$. A numerically stable solution was never obtained using time steps as small as 0.1×10^{-6} sec. The results obtained using the Runge-Kutta solution suggest that by reducing the time step even further, a stable solution could possibly have been obtained. These small time increments were not used since the amount of computer time required to obtain a solution to a problem would render the method impractical.

Houbolt Method vs Chan, Cox, and Benfield Routine with $\beta = \frac{1}{4}$

To determine the most advantageous numerical method of solution for use in the computer code, a comparison was made of the responses obtained using the method of Chan, Cox, and Benfield[20] ($\beta = \frac{1}{4}$) and Houbolt's method. The shell selected to serve as a test problem for the two numerical methods is shown in Fig. 2. This cap-torus-cylinder configuration was subjected to a 50-psi internal pressure. The shell was idealized using 50 elements distributed so that a large number of elements was concentrated in the vicinity of the cap-torus intersection and near the torus-cylinder intersection. With this element distribution, the size of the elements varies extensively. The widely varying element size coupled with the irregular shape of the shell provide a real and critical test of the numerical methods.

Using the zero harmonic, the displacements and stresses were calculated utilizing both numerical methods with single-precision numerical accuracy. By considering the results presented in Fig. 2, it can be concluded that the stresses calculated using both numerical methods are in good agreement. Thus, the choice of the most advantageous method of solution can be made based upon economic considerations. The largest time increment which can be used for this problem by the Chan, Cox, and Benfield method[20] is 1×10^{-6} sec. Houbolt's method of solution is, however, stable for a time increment of 3×10^{-6} sec. Obviously, a substantial saving of computer time can be realized by using the numerical method of solution which utilizes the larger time step. In addition, the amount of computation time required per step is less for the Houbolt scheme than for the Chan, Cox, and Benfield routine. The saving in computer time becomes more pronounced as the degree of nonlinearity is increased.

Test Problem for Houbolt Solution Scheme

The problem selected to serve as a critical test of the Houbolt method of solution is the shallow spherical cap ($\lambda = 6$) with clamped edges depicted in Fig. 3. The geometric and material properties presented at the top of this figure are used throughout the analysis. The cap is excited by an instantaneously applied load which is concentrated at the apex of the shell.

This particular problem was selected for two reasons. First, the problem is highly nonlinear. Using a 40-lb load, the displacements predicted by a nonlinear analysis are more than four times larger than the displacements predicted by a linear analysis. Second, the singularity which exists at the apex of this shell gives rise to extremely large terms in the structural stiffness matrix. The corresponding terms in the mass matrix are rather small. The net effect of a large stiffness to mass ratio is to give a speed of sound in the element which is very large. Since some of the stability criteria developed in the finite difference approach (Refs. 11, 14, and 28) are based upon the time required for a signal to travel from one mesh point to another, applying these criteria to this problem results in the prediction of an extremely small time increment. The same effect is produced by using very small elements.

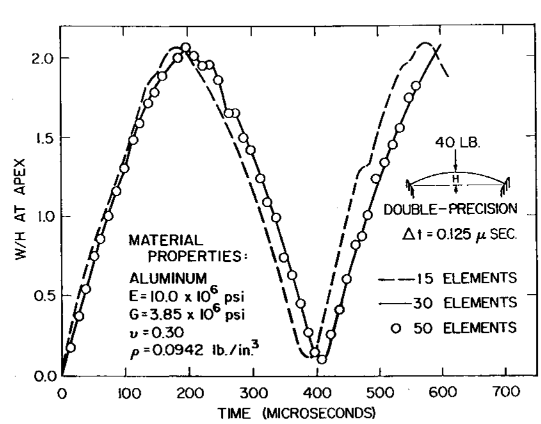

Fig. 3 Solution convergence with finite element idealization.

The following observations were made using this test problem and Houbolt's method.

1) Single-vs double-precision: it was found that double-precision is needed on the IBM 360/65 for highly nonlinear problems.

2) Load extrapolation procedure: first and second-order approximations were used to estimate the loads at time increment $n + 1$. It was found that the linear extrapolation procedure is more stable and yields results as good as those obtained with a second-order extrapolation.

3) Effect of time increment: for a 40-lb load at the apex, the problem was run with time increments of 0.25×10^{-6}, 0.125×10^{-6} and 0.04×10^{-6} sec. The results for the displacements were the same in all three cases. The solution showed a numerical instability for a time increment of 0.5×10^{-6} sec.

4) Convergence with improved finite element idealization: the test problem was run using 15, 30, and 50 finite elements and the results for the displacement at the apex vs time are shown in Fig. 3. It is noted that the 30, and 50 element cases yield the same results.

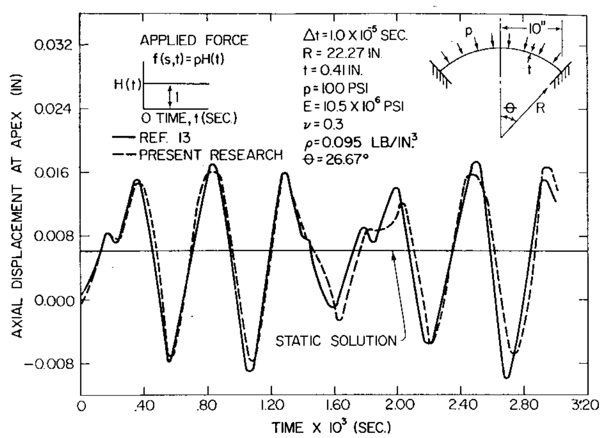

Fig. 4 Shallow spherical cap under axisymmetric dynamic loading.

Applications

The purpose of this section is 1) to present a comparison of current findings with other theoretical and experimental results; and 2) to present solutions to problems that will demonstrate the capabilities of the computer code.

The first example, as shown in Fig. 4, employs the shallow shell and the axisymmetric loading described by Klein and Sylvester.[19] The results have been verified by Popov using the normal mode superposition technique.

Klein and Sylvester present a linear analysis based on conical frustum elements and the numerical integration scheme described in Ref. 20. The formulation also makes use of a mass matrix based on energy principles but does not include the effects of rotary inertia. These effects are not significant for the problem under consideration. The time step of 1×10^{-5} sec and the 30-element idealization used in Ref. 19 were used in this research.

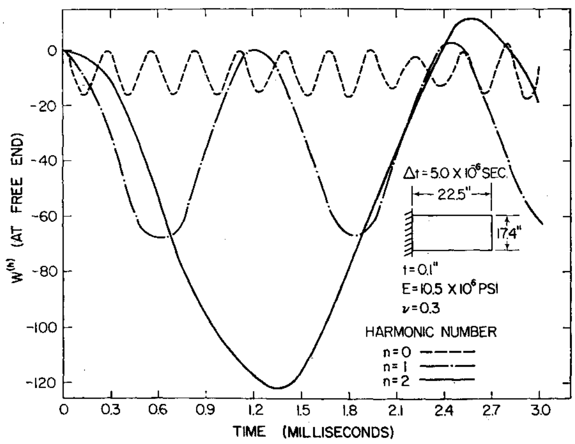

Fig. 5 Nondimensional Fourier coefficient of normal displacement vs time for cylinder under asymmetrical loading.

An investigation of Fig. 4 reveals that the agreement is quite good and the effect of nonlinearities is not significant. The slight discrepancies at the higher times can conceivably be attributed to the differences in formulation and method of solution or the fact that double-precision arithmetic is employed by Klein and Sylvester.

The second example involves the cylindrical shell described in Ref. 28 having geometric and material properties typical of those used in the missile industry. The structure is subjected to a blast loading and requires the use of the 0, 1, and 2 Fourier harmonics. Figure 5 shows a plot of time history of the Fourier coefficients of normal displacement at the free end of the cylinder. The results obtained are identical to the ones presented in Ref. 28. Houbolt's solution procedure with a time increment of 5×10^{-6} sec was used in the solution.

The third example illustrates the versatility of the computer code and solves the important problem of the symmetric buckling of shallow spherical caps under a step pressure loading. The problem has been investigated by other researchers,[31–33] and most results are now in good agreement.

The shell selected for the study is the one studied experimentally in Ref. 34 with different values of the shallow shell parameter being obtained by varying the thickness. The results are depicted in Fig. 6 and were obtained by using 30 elements and the numerical integration scheme presented in Ref. 20 with $\beta = \frac{1}{4}$; however, a check has been made using Houbolt's method and the results are the same.

The problem again reveals the advantages of the Houbolt method which required a time increment of 1×10^{-6} sec; whereas the method of Chan, Cox, and Benfield required a

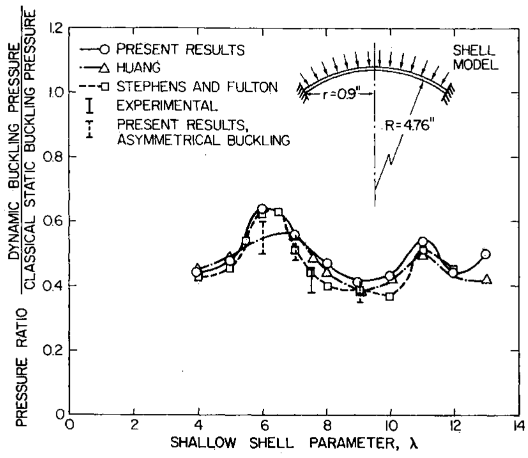

Fig. 6 Critical pressure ratio as a function of the shallow shell parameter.

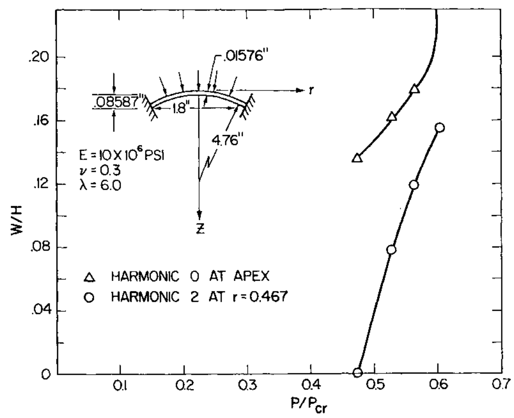

Fig. 7 Peak response of harmonic 0 and 2 for different pressure ratios.

time increment of 0.125×10^{-6} sec. Thus, for this problem Houbolt's method is more than eight times as efficient as the method of Ref. 20.

The curves shown in Fig. 6 reveal that the present results and those presented in Refs. 32 and 33 are in good agreement. A more detailed discussion of this problem is given in Ref. 21.

The fourth application of the program concerns the solution of a problem that has never been previously solved. This problem is the one of asymmetrical buckling of a shallow cap under a step pressure loading. The shell used in the study has the same basic geometry as the one used in the third example but has a thickness corresponding to a shallow shell parameter λ of 6.

The response of four Fourier harmonics was investigated by both Houbolt's method and the method of Ref. 20 and the results were the same. In one case the 0, 1, and 2 harmonics were used and in the second case the 0, 2, and 3. Both cases revealed that for the case of $\lambda = 6$, there is no build up in the first or third Fourier harmonics, and it is the second harmonic that reaches relatively large displacements. The same phenomenon has previously been observed in the static case.

The loading consisted of a constant uniform step pressure over the entire shell except for a slight increase over a circumferential angle of 4°. It was necessary to do this in order to excite the first, second and third Fourier harmonics.

Figure 7 shows how the displacements for the second harmonic can build up to values having the same order of magnitude of those of the symmetric component and at some critical time the two combine to give a very large displacement and enable us to define a buckling load.

The dynamic buckling pressure may be obtained from Fig. 7. It is seen from this figure that buckling occurs at $P/P_{cr} = 0.604$ as compared with 0.64 for symmetrical buckling. However, it is observed from Fig. 7 that the second harmonic is excited appreciably for all values of P/P_{cr} above 0.5. Thus, the threshold value is 0.5. This threshold value has not been shown to be a buckling load, but it is conceivable that if the calculations were carried for a large enough period of time buckling might occur. At most, the use of the threshold value is slightly conservative. The possibility of asymmetrical buckling is depicted in Fig. 6 as any value of $P/P_{cr} > 0.5$.

The fifth example (Fig. 8) demonstrates the feasibility of the finite element method for the analysis of wave propagation in shells of revolution. This example solves the problem of a cylindrical bar having a length of 24 in., radius of 6 in., and a wall thickness of 0.1 in. The cylinder was assumed to be fixed at one end and free at the other with the free end being subjected to a uniformly distributed axial pressure of infinite duration having a value of 100 psi. The solution was performed using Houbolt's method in double-precision arithmetic, a time increment of 1×10^{-6} sec, and 50 finite elements. The element breakdown was 10 of 0.24 in. in length, 10 of

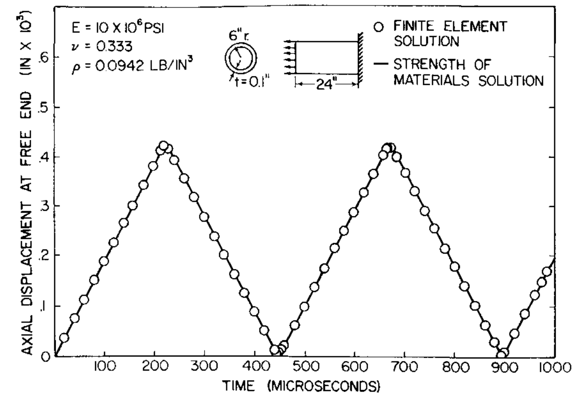

Fig. 8 Displacement response for a cylinder subjected to suddenly applied axial load.

0.48 in., 10 of 0.96 in., 10 of 0.48 in., and 10 of 0.24 in. in length.

The exact solution is obtained from elementary wave mechanics. The speed of sound in the material is given by

$$V_c = [E/(1 - \nu^2)\rho]^{1/2} \tag{23}$$

Substituting the material properties in Eq. (23) yields a speed of sound of 214,749 in./sec. Thus, an expansion wave travels down the cylinder at the prescribed speed. The theoretical stress behind the wave is 100 psi with zero stress existing in front of the wave. When the wave reaches the wall, it is reflected as an expansion wave that travels back down the cylinder. After the time required for the wave to transverse the cylinder in both directions, the state of stress is a constant value of 200 psi. The expansion wave is reflected from the free end as a compressive wave which reduces the stress to 100 psi and back to zero after reflection from the fixed end. This behavior gives displacement of a saw-tooth nature as shown in Fig. 8 along with the finite element results. It is noted that the agreement is excellent.

Figure 9 presents the meridional stress along the length of the cylinder after 50 μsec. After this period of time, the wave has travelled through the two changes in length in the finite element idealization. It is noted that the finite element and wave theory results are in good agreement. This example indicates that the damping in Houbolt's procedure is quite small.

The solution of the sixth example problem was performed for the purpose of checking out the code for multiple harmonics. The shell selected for this example was a spherical cap with a radius of curvature of 60 in., a base radius of 4.28 in., and a thickness of 0.125 in. The loading was localized as shown in Fig. 10 and was applied over a 2-in. radius circle with the center 3° from the apex. The solution was obtained using 28 elements and the first five Fourier harmonics. The method of Ref. 20 with a time increment of 0.25×10^{-6} sec was used in the solution.

Figure 10 is a plot of the meridional stress resultant as a function of time. It is noted that the dynamic solution oscillates about the static results. An exact solution is not available for the problem.

Computer Programs

The analysis and numerical solutions described herein have been programed in double-precision arithmetic in the FORTRAN IV language and carried out on an IBM 360/65 computer. For computational efficiency, the computer code is logically separated into two parts. The first code, called SAMMSOR I (Stiffness And Mass Matrices of Shells Of Revolution), accepts a description of the structure, generates stiffness and mass matrices, and writes them on tape for input to the second code, DYNASOR II (Dynamic Nonlinear

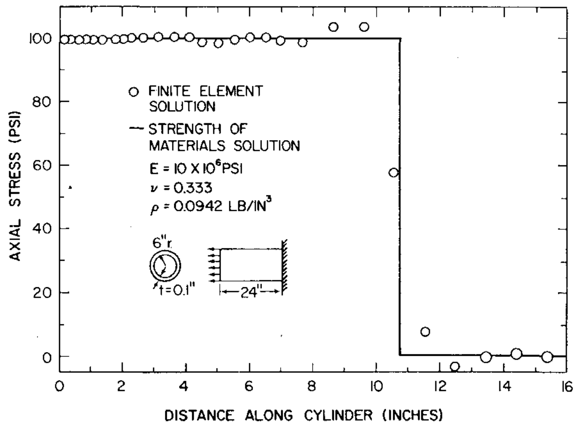

Fig. 9 Axial stress distribution along cylinder at 50.0 μ-sec.

Analysis of Shells Of Revolution). DYNASOR II generates generalized forces from a mechanical and thermal load history, reads the stiffness and mass matrices from tape, and then solves the initial value problem based upon given initial displacements and velocities.

The mechanical load history is described by specifying the pressure distribution over the element at discrete time intervals with a linear variation being assumed between the specified times. For a particular element, the pressure distribution is assumed to be constant in the meridional direction and to vary as a step function in the circumferential direction. In addition, the coding is capable of accepting concentrated ring loadings at each node and thermal loadings for each element.

The computer code has a restart provision permitting the program to be restarted at a particular time increment once the program has been run up to that time increment. The program allows restart information to be placed on tape periodically during the execution of DYNASOR II. If subsequent analysis of the output indicates that a smaller time increment is needed, the program can be automatically cycled to any time increment for which restart information is stored on tape and then the analysis restarted with a smaller time increment. This restart feature can save a considerable amount of time, particularly in buckling analyses.

The program output consists of all input control words, input loads and temperatures, generalized forces, stiffness and mass matrices, and the resultant displacements, stresses, and stress resultants. The displacements, stresses, and stress resultants are printed at all or any of the time increments specified and for as many circumferential angles as desired.

The program, as written for the IBM 360/65 computer, allows a solution using up to fifty elements and five Fourier

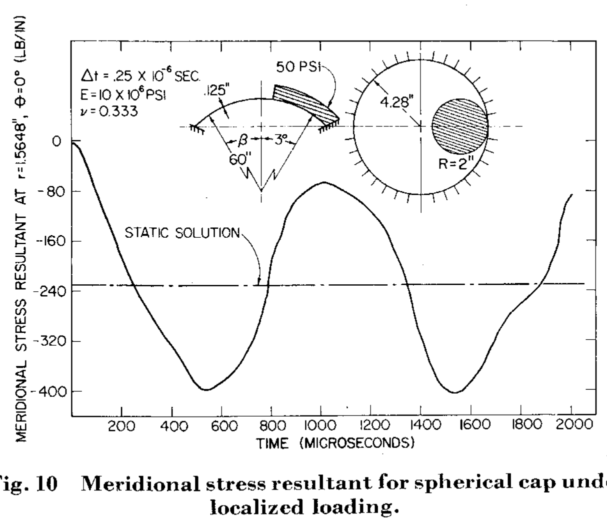

Fig. 10 Meridional stress resultant for spherical cap under localized loading.

harmonics. In double-precision, SAMMSOR I requires approximately 96,000 bytes of storage; whereas DYNASOR II requires 282,000 bytes. Considering the complexity of the computer program, it is extremely efficient. For example, the single-precision solution to the problem in Fig. 5, using 30 elements and three harmonics, was obtained in 13 min. The double-precision solution to the problem in Fig. 8 using one harmonic and 50 elements required 7 min. In double-precision, approximately 0.4 sec of computer time are required per time cycle using one Fourier harmonic and 50 elements. For five harmonics and 50 elements, 4 sec are required per time cycle. Few moderately nonlinear problems will require more than thirty minutes of computer time on the IBM 360/65.

Conclusions

A formulation and computer code has been developed which allows the solution of problems in the nonlinear dynamic analysis of shells of revolution in reasonable periods of time on the computer. Use of the computer code has been demonstrated through the solution of a wide class of difficult and practical problems.

In the formulation, the nonlinear terms are taken to the right-hand side of the equations of equilibrium and treated as additional generalized forces. These forces are evaluated under the assumption that all displacements may be represented by linear functions in the meridional distance, s.

The method of solution which proved to be the most stable is Houbolt's method with the nonlinear terms being determined by a first-order Taylor's expansion.

Undoubtedly, the use of a Taylor's expansion contributes to making the method unstable for large time increments, but in spite of this, Houbolt's method is more stable than the other numerical methods which do not require an extrapolation of the loads.

References

[1] Turner, M. J. et al., "Large Deflections of Structures Subjected to Heating and External Loads," *Journal of Aerospace Science*, Vol. 27, No. 2, Feb. 1960, pp. 97–107.

[2] Martin, H. C., "Finite Element Formulation of Geometrically Nonlinear Problems," *Proceedings, Japan-U.S. Seminar on Matrix Methods in Structural Analysis and Design*, Tokyo, Japan, August 25–30, 1969.

[3] Oden, J. T., "Finite Element Applications in Nonlinear Structural Analysis," *Proceedings, Conference on Finite Element Methods*, Vanderbilt University, Nashville, Tenn., Nov., 1969.

[4] Stricklin, J. A. et al., "Nonlinear Analysis of Shells of Revolution by the Matrix Displacement Method," *AIAA Journal*, Vol. 6, No. 12, Dec. 1968, pp. 2306–2312.

[5] Witmer, E. A. et al., "Larger Dynamic Deformations of Beams, Rings, Plates, and Shells," *AIAA Journal*, Vol. 1, No. 8, Aug. 1963, pp. 1848–1857.

[6] Krieg, R. D. and Duffey, T. A., "UNIVALVE II-A Code to Calculate the Large Deflection Dynamic Response of Beams, Rings, Plates and Cylinders," SC-RR-68-303, Oct. 1968, Sandia Laboratories, Albuquerque, N. Mex.

[7] Duffey, T. A. and Key, S. W., "Experimental-Theoretical Correlations of Impulsively Loaded Clamped Circular Plates," SC-RR-69-1225, June 1969, Sandia Laboratories, Albuquerque, N. Mex.

[8] Krieg, R. D., Duffey, T. A., and Key, S. W., "The Large Deflection Elastic-Plastic Response of Impulsively Loaded Beams: A Comparison Between UNIVALVE Computations and Experiment," SC-RR-68-226, July 1968, Sandia Laboratories, Albuquerque, N. Mex.

[9] Balmer, H. A. and Witmer, E. A., "Theoretical-Experimental Correlation of Large Dynamic and Permanent Deformations of Impulsively Loaded Simple Structures," FDL-TDR-64-108, July 1964, Massachusetts Institute of Technology, Aeroelastic and Structures Research Laboratory, Cambridge, Mass.

[10] Leech, J. W., Witmer, E. A., and Pian, T. H. H., "Numerical Calculation Technique for Large Elastic-Plastic Transient Deformation of Thin Shells," *AIAA Journal*, Vol. 6, No. 12, Dec. 1968, pp. 2352–2359.

[11] Wrenn, B. G., Sobel, L. H., and Silsby, W., "Nonsymmetric and Nonlinear Response of Thin Shells," LMSC B-72-67-3, Dec. 1967, Lockheed Missiles and Space Co., Palo Alto, Calif.

[12] Leech, J. W., Hsu, P. T., and Mack, E. W., "Stability of a Finite-Difference Method for Solving Matrix Equations," *AIAA Journal*, Vol. 3, No. 11, Nov. 1965, pp. 2172–2173.

[13] Johnson, D. E., "A Proof of the Stability of the Houbolt Method," *AIAA Journal*, Vol. 4, No. 8, Aug. 1966, pp. 1450–1451.

[14] Krieg, R. D., "Numerical Stability of a Finite Differencing of the Nonlinear Underwater Taut String Problem," SC-TM-69-265, June 1969, Sandia Laboratories, Albuquerque, N. Mex.

[15] Nickell, R. E., "On the Stability of Approximation Operators in Problems of Structural Dynamics," MM 69-4116-14, 1969, Bell Telephone Laboratories, Whippany, N.J.

[16] Stricklin, J. A., Navaratna, D. R., and Pian, T. H. H., "Improvements of the Analysis of Shells of Revolution by the Matrix Displacement Method," *AIAA Journal*, Vol. 4, No. 11, Nov. 1966, pp. 2069–2072.

[17] Grafton, P. E. and Strome, D. R., "Analysis of Axisymmetric Shells by the Direct Stiffness Method," *AIAA Journal*, Vol. 1, No. 10, Oct. 1963, pp. 2343–2347.

[18] Novozhilov, V. V., *Foundations of the Nonlinear Theory of Elasticity*, Graylock Press, Rochester, N.Y., 1956.

[19] Klein, S. and Sylvester, R. J., "The Linear Elastic Dynamic Analysis of Shells of Revolution by the Matrix Displacement Method," TR-66-80, 1966, pp. 299–329, Air Force Flight Dynamics Laboratory, Wright-Patterson Air Force Base, Ohio.

[20] Chan, S. P., Cox, H. L., and Benfield, W. A., "Transient Analysis of Forced Vibrations of Complex Structural-Mechanical Systems," *Journal of Royal Aeronautical Society*, Vol. 6, July 1962, pp. 457–460.

[21] Stricklin, J. A. and Martinez, J. E., "Dynamic Buckling of Clamped Spherical Caps Under Step Pressure Loadings," *AIAA Journal*, Vol. 7, No. 6, June 1969, pp. 1212–1213.

[22] Houbolt, J. C., "A Recurrence Matrix Solution for the Dynamic Response of Elastic Aircraft," *Journal of Aeronautical Science*, Vol. 17, Sept. 1950, pp. 540–550.

[23] Ambartsumian, S. A., "Theory of Anisotropic Shells," TT F-118, May 1964, NASA, p. 53.

[24] Zienkiewicz, O. C. and Cheung, Y. K., *The Finite Element Method in Structural and Continuum Mechanics*, McGraw-Hill, New York, 1967, pp. 24–25.

[25] Mebane, P. M., "An Improved Shell of Revolution Element Utilizing Cubic Displacement Functions," Master's thesis in Aerospace Engineering, 1970, Texas A&M University, College Station, Texas.

[26] Tillerson, J. R., "Numerical Methods of Integration Applied in the Nonlinear Dynamic Analysis of Shells of Revolution," Master's thesis in Aerospace Engineering, 1970, Texas A&M University, College Station, Texas.

[27] Levy, S. and Kroll, W. D., "Errors Introduced by Finite Space and Time Increments in Dynamic Response Computation," *Proceedings, First U.S. National Congress of Applied Mechanics*, June 1951, pp. 1–8.

[28] Johnson, D. E. and Greif, R., "Dynamic Response of a Cylindrical Shell: Two Numerical Methods," *AIAA Journal*, Vol. 4, No. 3, March 1966, pp. 486–494.

[29] Newmark, N. M., "A Method of Computation for Structural Dynamics," *Proceedings of ASCE*, 85, EM3, 1959, pp. 67–94.

[30] Hildebrand, F. B., *Introduction to Numerical Analysis*, McGraw-Hill, New York, 1956, p. 238.

[31] Simitses, G. J., "Axisymmetric Dynamic Snap-Through Buckling of Shallow Spherical Caps," *AIAA Journal*, Vol. 5, No. 5, May 1967, pp. 1019–1021.

[32] Huang, N. C., "Axismmetric Dynamic Snap-Through of Elastic Clamped Shallow Spherical Shells," *AIAA Journal*, Vol. 7, No. 2, Feb. 1969, pp. 215–220.

[33] Stephen, W. B. and Fulton, R. E., "Axisymmetric Static and Dynamic Buckling of Spherical Caps Due to Centrally Distributed Pressures," *AIAA Journal*, Vol. 7, No. 11, Nov. 1969, pp. 2120–2126.

[34] Lock, M. H., Okubo, S., and Whittier, J. S., "Experiment on the Snapping of a Shallow Dome Under a Step Pressure Load," *AIAA Journal*, Vol. 6, No. 7, July 1968, pp. 1320–1326.